UNLV | UNIVERSITY LIBRARIES

UNLV Theses, Dissertations, Professional Papers, and Capstones

2009

Metal induced crystallization of silicon thin films

Sandeep Kumar Raju Sangaraju
University of Nevada Las Vegas

Follow this and additional works at: https://digitalscholarship.unlv.edu/thesesdissertations

 Part of the Electrical and Computer Engineering Commons, Materials Science and Engineering Commons, and the Nanoscience and Nanotechnology Commons

Repository Citation

Sangaraju, Sandeep Kumar Raju, "Metal induced crystallization of silicon thin films" (2009). *UNLV Theses, Dissertations, Professional Papers, and Capstones*. 163.
http://dx.doi.org/10.34917/1392695

This Thesis is protected by copyright and/or related rights. It has been brought to you by Digital Scholarship@UNLV with permission from the rights-holder(s). You are free to use this Thesis in any way that is permitted by the copyright and related rights legislation that applies to your use. For other uses you need to obtain permission from the rights-holder(s) directly, unless additional rights are indicated by a Creative Commons license in the record and/or on the work itself.

This Thesis has been accepted for inclusion in UNLV Theses, Dissertations, Professional Papers, and Capstones by an authorized administrator of Digital Scholarship@UNLV. For more information, please contact digitalscholarship@unlv.edu.

METAL INDUCED CRYSTALLIZATION OF SILICON THIN FILMS

by

Sandeep Kumar Raju Sangaraju

Bachelor of Technology
J.N.T University
Hyderabad, India
2007

A thesis submitted in partial fulfillment of
the requirements for the

Master of Science Degree in Electrical Engineering
Department of Electrical and Computer Engineering
Howard R. Hughes College of Engineering

Graduate College
University of Nevada, Las Vegas
December 2009

Copyright by Sandeep Kumar Raju Sangaraju 2010
All Rights Reserved

UNLV
UNIVERSITY OF NEVADA LAS VEGAS

THE GRADUATE COLLEGE

We recommend that the thesis prepared under our supervision by

Sandeep Kumar Raju Sangaraju

entitled

Metal Induced Crystallization of Silicon Thin Films

be accepted in partial fulfillment of the requirements for the degree of

Master of Science
Electrical Engineering

Biswajit Das, Committee Chair

Yingtao Jiang, Committee Member

Mei Yang, Committee Member

Frank van Breukelen, Graduate Faculty Representative

Ronald Smith, Ph. D., Vice President for Research and Graduate Studies
and Dean of the Graduate College

December 2009

ABSTRACT

Metal Induced Crystallization Of Silicon Thin Films

by

Sandeep Kumar Raju Sangaraju

Dr. Biswajit Das, Examination Committee Chair
Professor of Electrical and Computer Engineering
University of Nevada, Las Vegas

Low temperature crystallization of thin film silicon is important for many industrial applications including flat panel displays and silicon thin film solar cells. Unfortunately this remains a major challenge since crystallization temperature of silicon is above 1,000 degrees Celsius, thus limiting to substrates that can tolerate high temperatures. The inability to deposit crystalline thin films on glass substrates is the reason why flat panel display industry uses amorphous silicon for LCD active matrix displays. Thus the ability to deposit crystallized thin film silicon at low temperatures will have significant impact on thin film silicon applications. It has been observed that certain metals can lower the crystallization temperature of silicon; however, investigation in this area has been rather limited. This thesis investigates the effect of two different metals, aluminum and silver, on the dependence of crystallization temperature of silicon thin films and investigates the properties of such materials.

TABLE OF CONTENTS

LIST OF FIGURES

ACKNOWLEDGEMENTS

I would like to express my sincere gratitude to my academic advisor Dr. Biswajit Das, without whose inspiration, guidance and support this work would not been possible. I will never forget his encouragement, constant guidance, support and kindness.

I would also like to thank Dr. Yingtao Jiang, Dr. Mei Yang and the graduate college representative, Dr. Frank van Breukelen for serving on my graduate committee. I sincerely appreciate the help by Dr. Lihua and Wen Shen. I am thankful to the faculty and staff of the Electrical and Computer Engineering department for their assistance.

This section would not be complete without acknowledging my family, my source of inspiration in all times. I would like to thank my parents, Sanjeeva Raju and Sudha Rani, for all of their love, encouragement and support throughout my Master's program.

CHAPTER 1

INTRODUCTION

The crystallization of amorphous silicon (a-Si) is increasingly gaining interest for polycrystalline silicon devices such as thin film transistors (TFTs) and thin-film solar cells [1, 2]. In relation to solar cell devices, the crystallization of a-Si offers the opportunity for using low temperature, and therefore low-cost substrates which is vitally important for the reduction of the overall costs of solar cells. Most attention in the field of crystallization has been given to solid phase crystallization (SPC) [3] and laser crystallization (LC) [4]. But SPC suffers from long annealing times and rather high temperature while laser crystallization remains an expensive and complex process. Due to these problems, metal-induced crystallization (MIC) has been investigated as an alternative crystallization process for thin-film device fabrication [5], although the interaction of metal and a-Si has been studied for many years. Aluminum-induced crystallization is one of the most used techniques because it has the following advantages: simple processing, process temperature below 600°C, standard industrial fabrication technique, short crystallization time, and also due to the fact that Al has a low resistivity and a good adhesion to a-Si. In this work, Aluminum induced crystallization and Silver induced crystallization of a-Si has been investigated for a wide range of annealing temperatures (200^0C -1000^0C). The deposition of silicon on to the metals is done by Electron beam deposition. The silicon of thickness 400nm is deposited onto the metal of thickness 100nm. After the deposition the thin films are then annealed to different temperatures under nitrogen filled furnace. Due to annealing the metal gets induced into a-Si making it to crystallize. The crystallization process has been

investigated by two different techniques, namely X-ray diffraction (XRD), and Raman spectroscopy. The silver induced crystallization is done in two different ways. One, is the silicon layer deposition with 400nm thickness and the another one has a less thickness of 250nm. We see difference in both types of experiments.

1.1 Organization of Thesis

This thesis is organized into five chapters. Chapter 1 gives the introduction and brief idea about the thesis. Chapter 2 concentrates mainly on the Electron Beam deposition of silicon thin films and the equipment used for deposition. Chapter 3 explains the process of Metal induced crystallization. Chapter 4 explains the principle behind and how, X-Ray diffraction and Raman spectroscopy is used to study crystallization of materials. Chapter 5 describes the experimental procedure and discuss about the results obtained. Chapter 6 concludes the thesis and discuss about the future scope.

CHAPTER 2

THIN FILM DEPOSITION

2.1 Introduction

Thin films are thin material layers with thickness from several nanometers to a couple of micrometers. Thin films are used in many different applications. For example, metal films can be used as metal gate electrodes. And oxide films can be used as oxide insulators, in semiconductor manufacturing. Oxide films can also be used as optical coatings or transparent conductive electronode in Photovoltaic application or the flat panel display industry.

Ferromagnetic thin films can be used in hard drive fabrication. Carbide and nitride thin films can be used for hard coatings and high temperature resistant coatings in tools and the aerosphere industry.

Thin film deposition can be divided into several categories: chemical vapor deposition (CVD), physical vapor deposition (PVD) and others such as plating, solgel process, and spin coatings. Among these techniques, CVD and PVD are the most frequently used techniques.

2.2 Theory of vapor deposition

PVD is a method of depositing thin films by the condensation of a vaporized form of the target material onto various surfaces. The deposition methods involved in PVD are mainly pure physical processes, such as high temperature vacuum evaporation or plasma sputter bombardment. Although some of PVD processes, for instance reactive magnetron sputtering, also involve chemical reactions. The CVD processes usually involve chemical

reactions among the precursors, which react or decompose resulting in depositing a thin film on to the substrates. Some CVD processes, for example PECVD, may be accelerated by plasma.

CVD and PVD each have their respective advantages and disadvantages. The advantages of CVD processes include large area coatings for industry and often no need of vacuum conditions. The disadvantages of CVD often include a high reaction temperatures, lower density films, toxic gas precursors, and lower adhesion to the substrates compared with PVD. As a result, PVD techniques are in demand in more areas these days. For example, in the semiconductor industry, the CVD deposition for aluminum interconnection layers may not be able to satisfy the demand for 32 nm technology in the future. However, a PVD-based system would likely able to meet this need through improved film properties. In addition, PVD processes are often environmentally cleaner when compared to CVD processes. Here, PVD method, Thermal evaporation is reviewed to provide the reader with the relevant background.

2.3 Methods of Evaporation

In PVD system, thermal evaporation and sputtering technology is popular and widely used. Optics industries usually adapt Thermal Evaporation to produce their products. Thermal Evaporation method use high temperature to melt the target into vapor state. The atom or molecule of target is speed up by high temperature. These molecules pass through a vacuum space and condensation of a vaporized form takes at substrate surfaces. The vacuum is required to allow the molecules to evaporate freely in the chamber, and they subsequently condense on substrate surfaces. As the term "Thermal" indicated, the

thermal high temperature is the key role of this method. "Thermal High Temperature" is same for all evaporation technologies, only the techniques used to evaporate the target differs. Several techniques are used as the thermal high temperature means.

2.3.1 Resistive Heating

This method uses a big current passing through the resistor; the resistor will generate high temperature and melt the target material. The target material is usually attached on the resistor. Traditionally the resistors are made by Tungsten (W), Tantalum (Ta), Molybdenum (Mo) which is with very high melting temperature. The melting temperature of target is much lower than resistors. When the current pass, only the target gets melted or vaporized. And gets deposited on to the substrate surface.

The resistor can be made to different shapes depending on what amount of target you want to evaporate and the uniformity of evaporation. The wire (filament) is first to be used as resistor and attached with target. In some coating machine and target material requires, the boat or basket shaped resistor. Flash evaporation is used for two or more different materials in one coating procedure. Since different target material need different melting temperature, the resistor does not attach the target before melting temperature. It is empty. Once the temperature reach the working condition, the target will be attached to the resistor and evaporated immediately. Then other material target is attached to the resistor and evaporated. By this way, different materials could be manipulated and evaporated to same substrate, and make a multilayer thin films.

This technique has couple of advantages. Its equipment is relative simple and cheap. And the target (source material) could be made to different shape depending on the need. There are many drawbacks for this method such as: Since high temperature is generated

by resistor and conducted to target, the resistor material will react with the target and pollute the evaporation purity, thus harming the thin film quality. The speed of deposition is very slow.

2.3.2 Electron Beam Evaporation

High speed electron beam is used to hit the target material; the kinetic energy of the beam is transferred to thermal energy and creates high temperature on target material. The electron beam is generated by an electron gun, which uses the thermionic emission of electrons produced by a tantalum cathode. Emitted electrons are accelerated towards an anode with very high speed. The crucible in which the target is placed, acts as the anode. A magnetic field is also applied to bend the electron trajectory. The electron beam makes the target material to vaporize; this vapor is then condensed on the substrates forming a thin film. Fig. 2.1 shows the schematic diagram of electron beam evaporator. When the electron beam from electron gun focused by magnetic plates falls onto the source material, the kinetic energy of the beam is transformed to thermal energy and creates high temperature on source material. This in turn vaporizes the material and the vaporized material condenses on the substrate forming a thin layer.

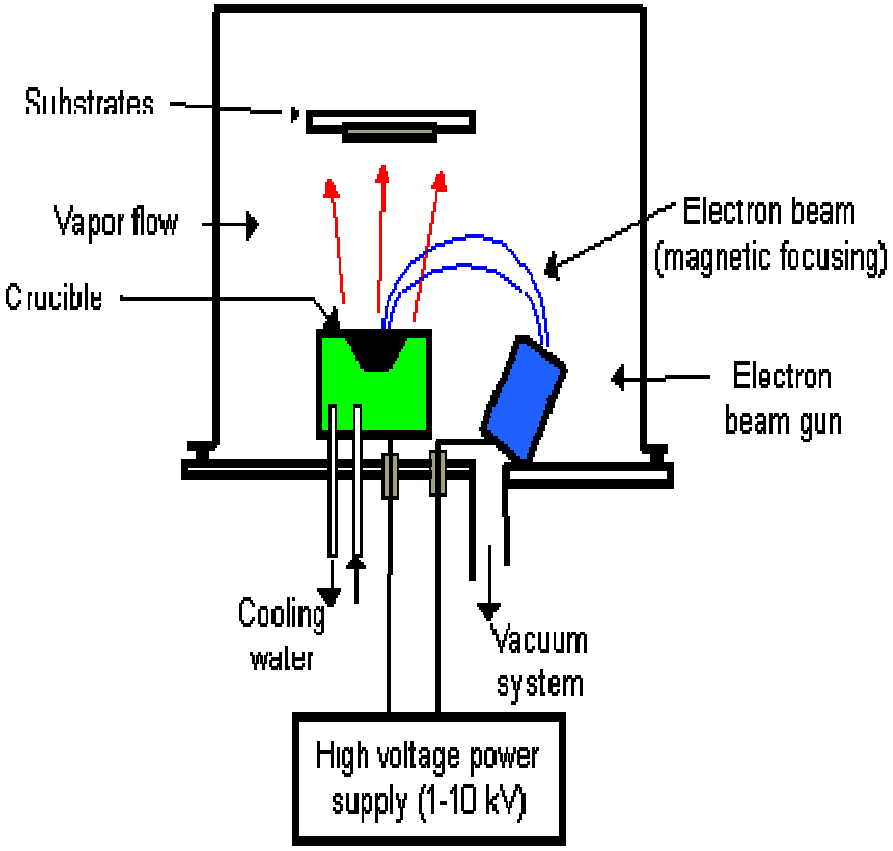

Figure 2.1 Schematic of Electron Beam Evaporator.

After 1968, Hanks developed an Electron Beam with 270° bending. This progress allowed the gun installed under the crucible. It hugely improved the target vapor contaminating the cathode tip and can prevent cathode failure.

Via the control of the magnetic mechanism (term "magnetic lens"), the electrons can be focalized and change its bombard position. It can obtain a much localized heating on the material to evaporate. It also allows controlling the evaporation rate, from low to very high values. Most important of all, it can deposit the materials with high melting point (W, Ta, C, dielectric oxide, etc.). Effective water cooling to crucible can avoid contamination problems, which will degasification undesired material in the coater.

Advantages:

- Using the water cooling to the crucible, the contamination due to the crucible material to the target vapor can be eliminated to the lowest level.
- Thin film purity is much higher than resistive heating.
- Dielectric Oxide target material could be deposited by this method.
- With different targets put in different crucibles which are installed in a circle, we can easily deposit different target film and make a multilayer deposition.
- With adequate adjustment of the electron bombard spot size, this method allows to increase the uniformity of film thickness.

Disadvantage:

- Inappropriate control of electron beam or electron flow may decompose or ionize the target. It may result material absorption or accumulating electron and arc to damage the quality of film surface.
- The electron beam gun needs large electric energy consumption. With a 10~15K Volt power consumption, it usually need to sustain several hours. This

characteristic makes this type of method to consume more energy than other methods.

Electron Beam Gun Evaporation Technology got its predominance position in Thermal Evaporation field since 1950's. With the progress of computer and automatic control skill, almost all multilayer optical thin films are made by this method in this modern era.

2.3.3 Laser Deposition

Using laser beam as a evaporation means. The laser can evaporate the target source by heat or photo dissociation. Without the electric charge accumulating, the film will not harm by electric effect. The laser beam is a focus energy beam, it do not disperse many through long distance. The target source can locate far compare to other means. This made contamination reduced to lowest level. However, laser is expensive equipment. The high cost of coater makes this method not popular to industry producer.

2.4 Components and Operation

Sharon Vacuum Electron Beam deposition system (Fig. 2.2) is used for evaporation and deposition on substrates. It’s a 24”x24”x18” chamber with four pocket 6kW electron beam gun. It has a PLC controlled automatic pumpdown, Dual shutters, Sycon deposition controller, CT-8 cryo pump, Water cooled rotary substrate stage. This e-beam evaporation system dedicated for evaporating titanium (Ti), gold (Au), nickel (Ni), silicon (Si), Aluminum (Al), Silver (Ag) and germanium (Ge) films. Other metals such as platinum (Pt) and Chromium (Cr) may also be incorporated. This system is cryo-pumped and attains a base pressure of less than 2e-7 Torr.

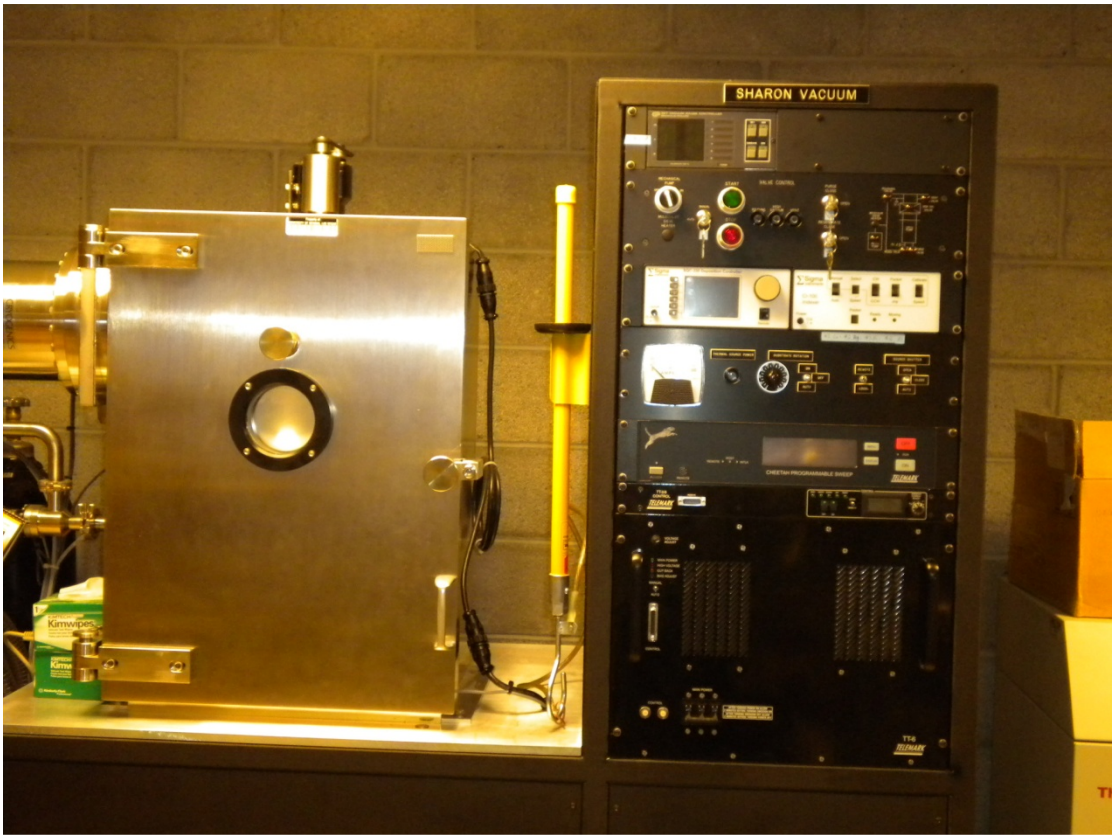

Figure 2.2 Sharon Vacuum Electron Beam deposition system.

E-beam evaporation uses an electron beam to heat source of material in crucible. Electrons are emitted from a heated filament and are accelerated to a high velocity by several kV. Electron current is typically small, around 100mA. A permanent, horseshoe magnet bends and guides the e-beam in a circular path from the filament to the source. The most common error is to have too much or too little material in the crucible. The crucible should be at least 1/3 full, but not more than 3/4 full. If there is not enough material, it is possible to burn a hole through the bottom of the crucible and supporting copper hearth. If there is too much material it can escape from the crucible and contaminate the system. Material can be added to the crucible as needed. For the cleanest

deposition, the beam current should be adjusted to just melt a spot in the middle of the material. If the power is too high, all the material will melt, and then the crucible material can diffuse into it. As power is increased and more material is melted, the deposition rate increases, but also the amount of spitting of droplets of material increases. You need to look through the glass to see if this is happening, and then find a compromise setting that minimizes spitting, but still gives a reasonable deposition rate.

CHAPTER 3

METAL INDUCED CRYSTALLIZATION

3.1 Introduction

Metal- induced crystallization (MIC) is a method by which amorphous silicon (a-Si), can be turned into polycrystalline silicon at relatively low temperatures. In MIC the metal is deposited on to a substrate, and then deposit an amorphous Si film on to the metal. The structure is then annealed at temperatures between 200°C and 1000 °C which causes the a-Si films to be transformed into polycrystalline silicon. Polycrystalline silicon thin films are attracting more interest in electronic devices such as thin film transistors, solar cells, and sensors in the recent years.

3.2 Principle of Operation

The process of MIC starts with the interaction between the metal and Si atoms. The difference in the electro negativity between the metal and the Silicon leads to redistribution of the electric charge of the metal-Si bonds closer to the metal atoms, and this change the position of the electrons around the neighboring Si-Si bonds. The electron pairs from electrons belonging to two neighboring Si atoms transform to electrons belonging to more than two neighboring Si atoms, i.e., the electrons in a-Si are no longer localized and they occupy delocalized orbital's. This changes the distance between the Silicon atoms because the Si-Si bonds weaken. The metal phase being responsible for loosening the covalent bonding in Silicon makes the amorphous phase unstable. The interface boundary between the metal and the a-Si layer is appropriate for a metal-Si interaction leading to the process of a-Si crystallization because of amorphous Silicon

imperfections - vacancies, dislocations and dangling bonds. During the isothermal heat treatment, the metal film is dissolved into the semiconductor film where it diffuses and precipitates.

The main difference between Aluminum Induced Crystallization (AIC) and Silver Induced Crystallization (SIC) is due to the different reaction behaviors of Al and Ag with Si. Ag and Al form a eutectic. A eutectic is the melting point of a mixture of two or more solids depends on the relative proportions of its ingredients. The initial step during the annealing of the Al/a- Si interface is dissolution of a-Si in Al (Fig 3.1 a), followed by diffusion of the Si solute through the metal (Fig 3.1 b). Due to weakening of covalent bonds of the a-Si, the diffusion of Si atoms into metal film takes place. Because of the continuous supply of Si atoms, the Si grains will continue to grow at these sites until they contact each other and form a continuous film. This results in layer inversion. For Al, this process can start immediately because of the solubility of Si in the metal film. But, for Ag this solubility is negligible even at high temperatures. This explains why Al is much more efficient in lowering the crystallization temperature than silver (Ag). The metal film is saturated with Si, the dissolved semiconductor becomes supersaturated and the super saturation can be relieved by crystallite growth. The mechanism of crystallization involves intermixing of Al and Si atoms (Fig 3.1 c) and the formation of an alloy of high metal concentration in the amorphous Crystalline interface**.** The Al layer with its crystal structure induces in the newly formed Si phase, a structural conformity with the crystalline phase. As a result, polycrystalline Si grains are formed. The Al atoms diffuse along the grain boundaries and segregate between them and outside of the poly-Si layer. The process of crystallization will stop when all of Al is repulsed at the a-Si and poly-Si

interfaces. This process of AIC is known as the aluminum-induced layer exchange process.

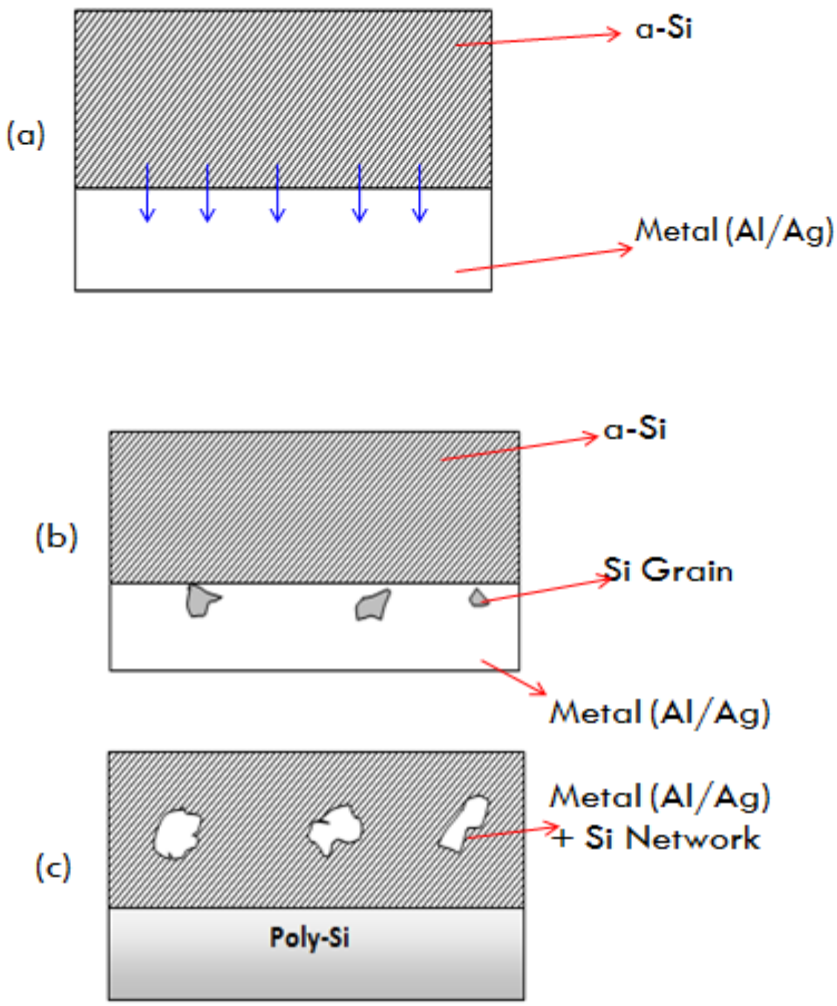

Figure 3.1 Overview of MIC process using eutectic reacting metals (Al, Ag).

3.3 Components and Operation

Lindberg/Blue M 1100°C box furnace is used for annealing of the samples. Due to heating of the samples on different temperatures in this furnace makes the metal layer to get induced into a-Si making it crystalline. This furnace features a choice of

microprocessor-based single set point or programmable control instrumentation. These furnaces include unique insulation and heating element composites to minimize outer surface temperatures while maintaining uniform heat distribution within the chamber. Controlled heat-up rate eliminates thermal shock to materials. It has quick heat-up and cool-down rates. The unique double wall construction minimizes exterior surface temperatures for operator safety and energy efficiency. Long life Type "K" thermocouple is used. This furnace has air vent and air inlet for inert gas. The main power on/off switch is on control panel. Safety door switch to interrupt power to heating element when door is opened; protects heating element and minimizes exposure to end-user. Microprocessor-based control with advanced self-tuning feature automatically sets best control parameters for the thermal process. PID control (proportional, integral, derivative) prevents overshoot. There is a simultaneous LED display of actual temperature vs. setpoint. It may be configured to display temperature in either °C or °F. This furnace works at 208/240V and 50/60Hz. The heat-up/cool-down graph for the furnace is shown in figure 3.2. This graph shows the time taken by the furnace to heat up and to cool down.

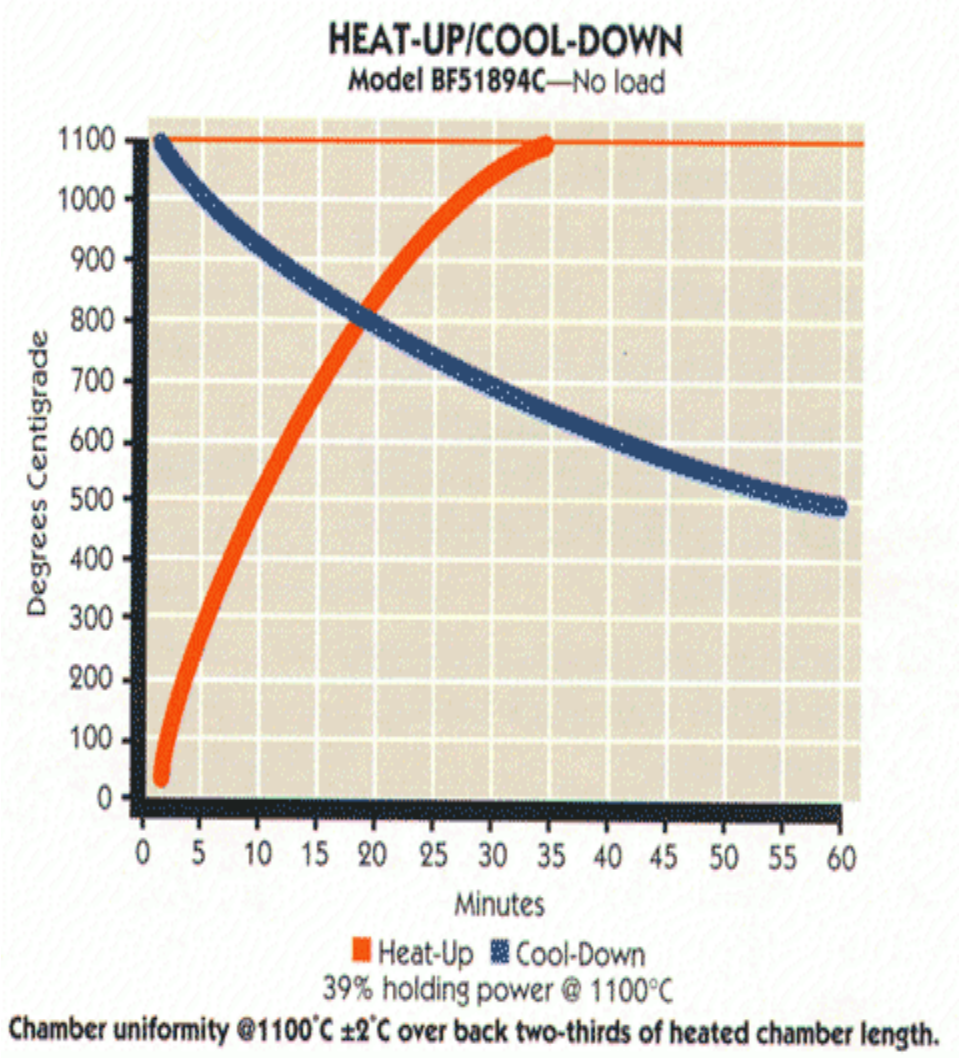

Figure 3.2 Lindberg/Blue M 1100°C box furnace heat-up/cool-down graph.

The operation of the furnace is explained into two parts. The first part is resetting the high temperature alarm setpoint and second part is resetting the local setpoint. First, for resetting the high temperature alarm, press and hold the SET/ENT button on the controller for three seconds until the display shows “mode RES”. Press and release the SET/ENT button to display “PrG 0”. Then press the UP/RESET button to show the lower display value “1”. Press and release the SET/ENT button until the high temperature alarm

setpoint value is displayed as “A1”. Select the alarm setpoint 5C above the target temperature (temperature for sample to be annealed at). Press and hold SET/ENT for three seconds to exit this menu. The second step for resetting the local setpoint, press and release the SET/ENT button until “mode” is displayed. At “mode” display, press the “UP” arrow button to make the lower display value to “LCL”. Press and release the SET/ENT button once to enter the local mode. Use the “UP” and “DOWN” buttons to select the operating temperature. At this point the power automatically turns on and the temperature is raised to the operating temperature. After the temperature in the furnace reaches the operating temperature and goes higher than the alarm setpoint, the power of the furnace automatically shutdowns and slowly the temperature lowers than the alarm setpoint. By following these steps the samples are annealed for one hour at different temperatures. The annealed samples are then studied using different techniques explained in the following chapter.

CHAPTER 4

THIN FILM CHARACTERIZATION

4.1 Introduction

The thin film crystallization is characterized by two of the techniques. One is X-Ray diffraction and other method used is Raman spectroscopy. This chapter briefly explains both the techniques and the principle behind these techniques.

4.2 X-Ray Diffraction

Solid matters can be categorized into amorphous and crystalline. In Amorphous materials the atoms are arranged in a random way. For example, Glasses are amorphous materials. In Crystalline materials, the atoms are arranged in a regular pattern, and there are smallest elements that by repetition in three dimensions describe the crystal. This smallest volume element is called a unit cell. About 95% of all solids are described as crystalline. X-Ray diffraction (XRD) is one of the most powerful techniques for qualitative and quantitative analysis of crystalline compounds. This technique provides information that cannot be obtained by any other ways. The information obtained includes degree of crystallinity, types and nature of crystalline phases present, amount of amorphous content & size and orientation of crystallites. The principle of operation for X-Ray diffraction technique and how it is used to characterize the solid matters is explained in the next section.

4.2.1 Principle of operation

An electron in an electromagnetic field will oscillate with the same frequency as the field. When an X-ray beam hits an atom, the electrons around the atom start to oscillate

with the same frequency as the incoming beam. In almost all directions we will have destructive interference. Destructive interference means the combining waves are out of phase and there is no resultant energy leaving the solid sample. In crystals the atoms are arranged in a regular pattern, and in a very few directions we will have constructive interference. The waves will be in phase and there will be well defined X-ray beams leaving the sample at various directions. Hence, a diffracted beam may be described as a beam composed of a large number of scattered rays mutually reinforcing one another.

X-ray diffraction employs electromagnetic waves with a wavelength on the order of 1 angstrom. Since wave diffraction occurs when the dimensions of the diffracting object are of the same order of magnitude as the wavelength of the incident wave. X-ray diffraction of semiconductor thin films is generally carried out in a diffractometer. The source of the X-rays is called an X-ray tube (Fig. 4.1). It consists of a water-cooled copper target onto which an accelerated electron beam is impinging inside a vacuum tube. Because of the Bremsstrahlung effect, X-rays are emitted with wavelengths that are characteristic of the copper element. Bremsstrahlung is the original German name for the effect of generation of X-rays via electron deceleration through its interaction with the Coulomb field of the nucleus. Through these inelastic interactions, X-rays are emitted which can have energies as high as the beam energy. These X-rays are then filtered and collimated into a beam through the use of a monochromator consisting of nearly perfect silicon crystals placed at specifically chosen angles to permit reflection of the X-rays. Diffracted waves from different atoms can interfere with each other and the resultant intensity distribution is strongly modulated by this interaction. If the atoms are arranged in a periodic fashion, as in crystals, the diffracted waves will consist of sharp interference

maxima (peaks) with the same symmetry as in the distribution of atoms. Measuring the diffraction pattern therefore allows us to deduce the distribution of atoms in a material.

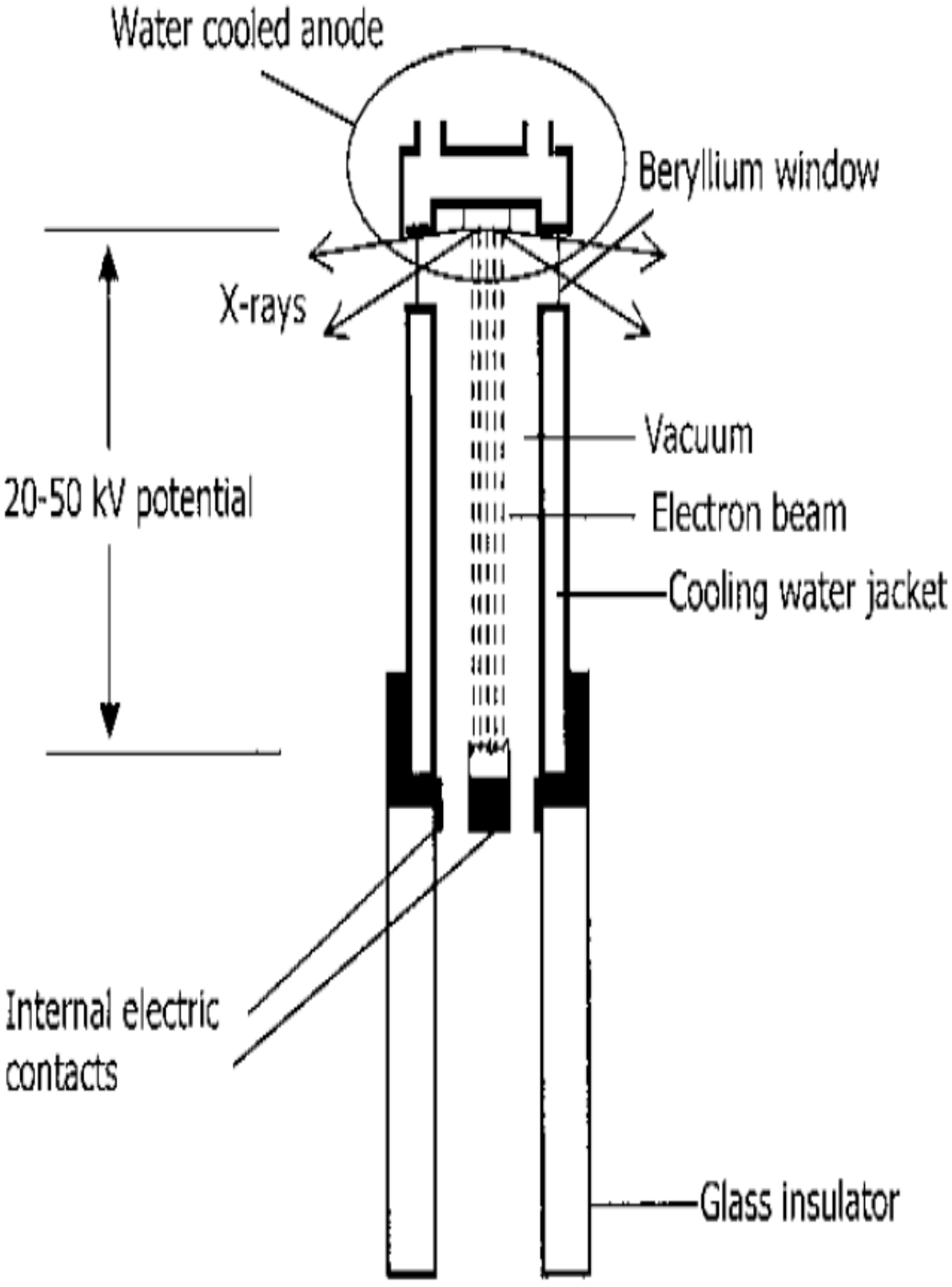

Figure 4.1 Schematic diagram of X-Ray tube used for X-Ray diffraction.

The peaks in an X-ray diffraction pattern are directly related to the atomic distances. For a given set of lattice planes with an inter-plane distance d, the condition for a diffraction (peak) to occur can be found using Bragg's law:

$$2d \sin\theta = n\lambda$$

Where θ is the incident angle, λ is the wavelength of the X-ray, and n is an integer representing the order of the diffraction peak. This process is shown schematically in Fig. 4.2.

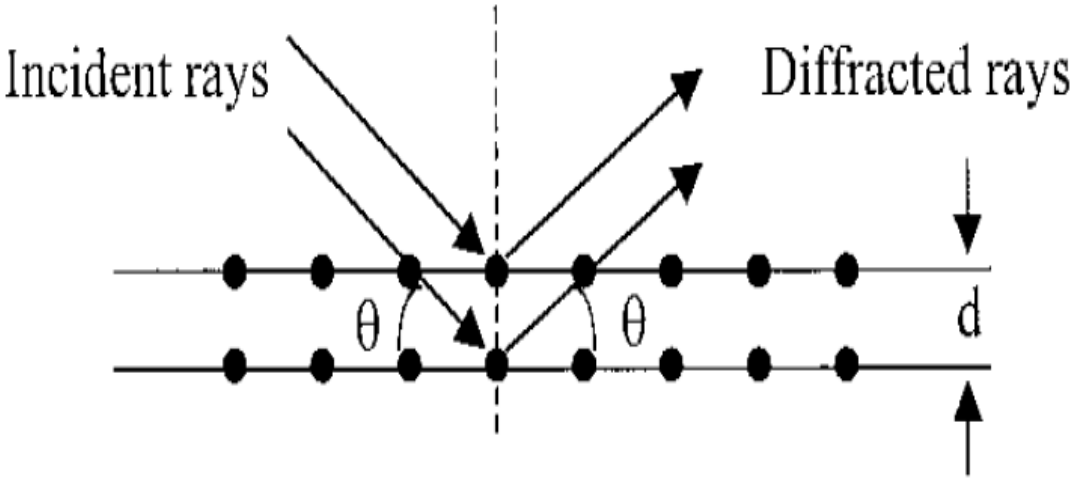

Figure 4.2 Schematic of diffraction of x-rays by a crystal.

Diffraction effects are observed when electromagnetic radiation impinges on periodic structures with geometrical variations on the length scale of the wavelength of the radiation. The interatomic distances in crystals and molecules amount to 0.15–0.4 nm which correspond in the electromagnetic spectrum with the wavelength of X-rays having photon energies between 3 and 8keV. Accordingly, phenomena like constructive and

destructive interference should become observable when crystalline and molecular structures are exposed to x-rays.

The advantages of X-Ray diffraction are:

- Detailed Phase analysis of materials can be done. Phase analysis like percent crystallinity in polymers and ceramic materials, structural characaterization and analysis of catalysts and chemicals and deatailed soil and clay mineral analysis.
- Quantitative analysis can be done like accurate phase quantification by Rietveld method, Crystallite size determination and Microstrain determination.
- Crystalline or Amorphous ratio determination can be obtained by a profile fitting technique.

4.2.2 Equipment Used

X'Pert PRO Diffractometer is used to study the crystallization of metal induced silicon thin films. The X-RAY sources present in this diffractometer are 3 kW Copper tube and 2 kW Cobalt tube. Few optic components used are Focusing and parallel PreFix optics, programmable slits, tunable diffracted beam monochromator. Detectors used are Xe proportional counter and solid state X'cellerator. The softwares used for analysis are Hi-Score search-match software, X'Pert Plus crystallographic analysis software with Rietveld capability and ProFit line profile analysis software. The picture below shows the equipment used for characterization of samples by X-Ray diffraction. X-Ray Diffraction an analysis is performed with an automated diffractometer and the data analyzed with a computerized least squares technique. A X'Pert PRO x-ray diffractometer, equipped with a graphite monochrometer and a copper tube is used to collect the thin films data. The

data is collected on a PC and analyzed using a computerized search and match procedure. The laboratory is also equipped with the JCPDS database.

Figure 4.3 X'Pert PRO X-Ray Diffractometer

4.3 Raman spectroscopy

4.3.1 Principle of Operation

When photons are incident upon a medium, they get scattered either elastically (Rayleigh scattering) or inelastically (Raman scattering). The scattering process without a change of frequency is called Rayleigh scattering, and this process is described by Lord Rayleigh and which accounts for the blue color of the sky. In Rayleigh scattering, the energy of the emitted photon is the same as the incident photon. On the other hand, in Raman scattering, the energies of the scattered and incident photons are different. A change in the frequency of the light is called Raman scattering. Raman shifted photons of light can be either of higher or lower energy, depending upon the vibrational state of the molecule. The energy change is depicted in Fig. 4.4, where an incoming photon either creates a phonon and is re-emitted at a lower energy (anti-Stokes scattering) or annihilates a phonon and is re-emitted at a higher energy (Stokes scattering). The inelastically scattered light can be collected, and information about the energy levels within the medium can be deduced from the energy change in the light. This process can also be easily explained. Most of the molecules are initially in the ground state but because of thermal agitation, some of the molecules will be in excited state. The scattering process can be explained as the incoming photon raises the molecule to a virtual (non-existent) excited state. But since the molecule cannot remain in this virtual level, it must immediately come back to a lower level with the emission of a photon. If the molecule falls into the same level as it started from, there is no frequency shift in emitted photon and this is called as Raleigh scattering. If the molecule falls into a different level, the energy of the emitted photon must differ from that of incoming photo

in order to conserve total energy, the emitted photon has a different frequency. This process is called Raman scattering. The frequency can decrease giving rise to Strokes lines in the spectrum or increase giving anti-Stokes lines. This depends on whether the molecule starts in the ground state or an excited state. The larger the Raman shift, the higher the excited state, and the less likely it is to be thermally populated. Therefore, anti-Stokes lines with small Raman shifts are likely to be observed.

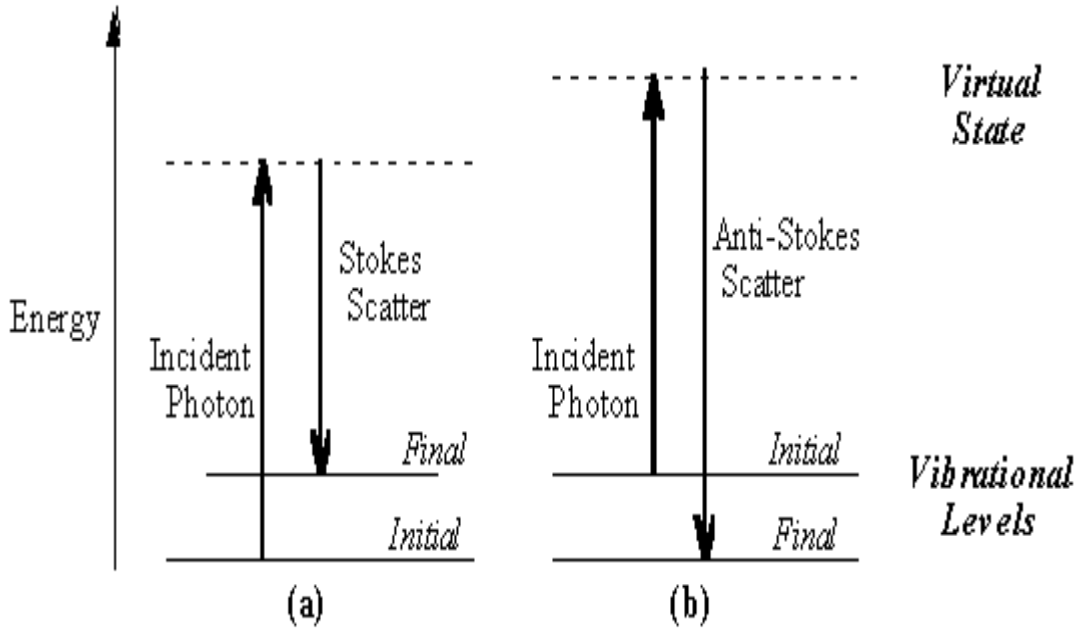

Figure 4.4 Schematic depiction of Raman scattering processes within a medium.

Spectroscopists and especially chemists, frequently use wave number to measure frequency. Wave number is expressed in units of reciprocal centimeters. A wave number is defined as $v* = {}^{v}/_{c} = 1/\lambda$, where c is the speed of light in cm/s and λ is the wavelength in cm. The wave number gives the number of wavelengths of light that will fit into one centimeter. A monochromatic light source, usually an argon ion laser, is used

to excite the sample and a spectrometer 1PMT set is used to detect the scattered light. Raman spectroscopy has become an important analytical and research tool. It can be used for applications as wide ranging as thin films, semiconductors, pharmaceuticals, polymers and carbon nano-materials. Raman spectroscopy is a light scattering technique, and can be explained as a process where a photon of light interacts with a sample to produce scattered radiation of different wavelengths. Raman spectroscopy is extremely rich in information. This information may be useful for chemical identification, characterization of molecular structures and effects of bonding.

Advantages of Raman spectroscopy:

There are various spectroscopic techniques, such as infrared spectroscopy and chromatography. These are used for chemical characterization. Infrared spectroscopic measurements can provide a wealth of information, but their sensitivity is not so high and substantial efforts may be needed to extract unambiguous information about the particles. In comparison, Raman Spectroscopy (RS) has the following advantages:

- RS is nondestructive and has rapid tool for structural characterization of crystalline, non-crystalline and amorphous materials.
- The sample preparation is much simpler for RS than compared to infrared.
- RS can provide higher sensitivity with comparable selectivity and chemical speciation.
- RS is equally useful for any state of matter, such as solid, liquid or gas, and can identify any type of organic, inorganic and biochemical species in solid, liquid or gas form.
- Most organic and inorganic molecules are Raman active.

4.3.2 Equipment Used

The Horiba Scientific product called Raman spectrometer LabRAM HR system is used to study the crystallization of the samples. The LabRAM HR system provides ultra high spectroscopic resolution. It also provides unique wavelength range capability. Due to these kinds of functionalities this system provides both great flexibility and high performance. It is an integrated, simple to use, and high stability bench-top instrument designed to undertake reproducible Raman measurements at high, medium or even low spectral resolution. The high resolution mode is uniquely ideal for subtle band analysis such as that for phase (crystalline/amorphous), or proteins, hydrogen and weak bonding forces and semiconductor stress measurements. Band analysis in the order of 0.3 cm^{-1} to 1 cm^{-1} is particularly suited to the HR mode. It is suitable for Raman, fluorescence and luminescence measurements. Multiple laser capability provides wavelength from visible to near IR. It has a unique adjustable angle notch filter technology.

CHAPTER 5

EXPERIMENTAL PROCEDURES, RESULTS AND DISCUSSIONS

5.1 Deposition

In the present work, we prepared the structure of a-Si/metal/sapphire and were processed through a rapid thermal process. The substrates used for this structure were of thickness 330Microns and with a diameter of 2 inch. To study metal induced crystallization of silicon thin films, we made few samples with two different metals Aluminum and Silver. These samples were made by evaporating the metals and depositing onto the substrate. To make the samples, the metals (AL, Ag) have to be deposited on to the substrate first and then on the top of metal layer, silicon layer is deposited. Sharon vacuum Electron beam deposition system is used for all thin film depositions. Deposition by this system takes place under very high vacuum with pressure below 4e-6 Torr. Three different samples were made. First, the substrate was deposited by 100nm aluminum and then followed immediately by silicon layer of thickness 400nm (a-Si/Al/Sapphire). Fig 5.1 shows the schematic diagram of a-Si/Al/Sapphire. Second, Silver layer of thickness 100nm deposited on to substrate and followed by silicon of thickness 400nm (a-Si/Ag/Sapphire). Fig 5.2 shows the schematic diagram of a-Si/Ag/Sapphire. Third, substrate deposited with silver of thickness 100nm and silicon with 250nm (250nm a-Si/Ag/Sapphire). Fig 5.3 shows the schematic diagram of 250nm a-Si/Ag/Sapphire.

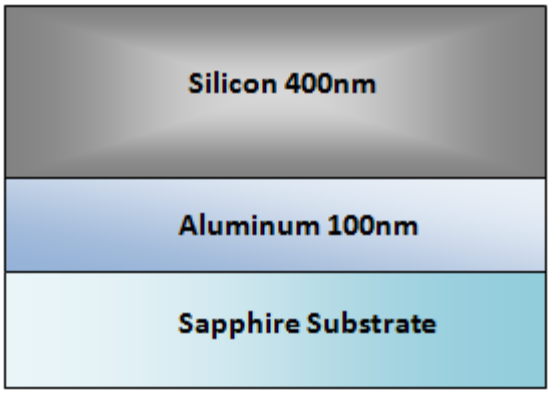

Figure 5.1 shows the schematic diagram of a-Si/Al/Sapphire.

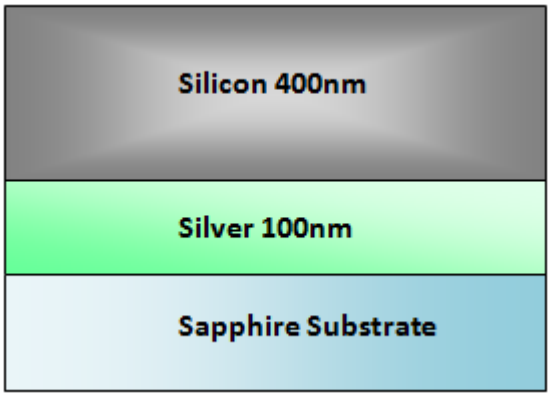

Figure 5.2 shows the schematic diagram of a-Si/Ag/Sapphire.

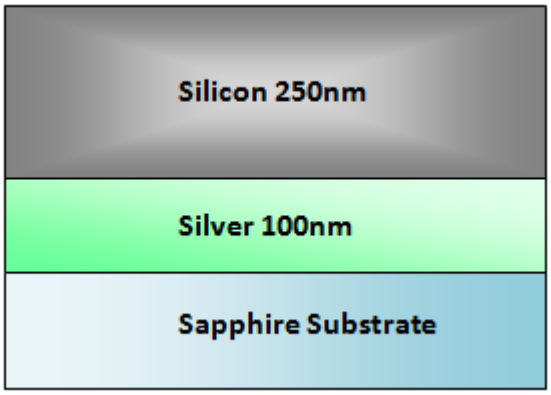

Figure 5.3 shows the schematic diagram of 250nm a-Si/Ag/Sapphire.

The data of deposition by E-beam evaporator for different samples are given in tables below. All the experiments were done with spacer underneath the crucibles and the sweep was turned ON. The crucibles were filled with the target materials first and then placed inside the Evaporator. Let us discuss about a-Si/Al/Sapphire deposition. The target materials for this sample are Aluminum and silicon. So, one of the crucible was filled with aluminum and other with silicon and placed in the evaporator. Place a substrate on to the substrate holder. First, deposit the aluminum layer of thickness 100nm by just evaporating the target material. Then just rotate the aluminum filled crucible position to silicon filled crucible by using the control switch and deposit silicon of 400nm on to the aluminum layer. Similarly, the other samples a-Si/Ag/Sapphire and 250nm a-Si/Ag/Sapphire can also be done. After the deposition by E-beam evaporator the samples obtained are made into eight parts of each sample. These small segments of samples were annealed at different temperatures from 200°C -1000 °C. The annealing was done in a Lindberg/Blue M 1100°C box furnace under nitrogen gas. All the samples were heated for one hour at different temperatures. One of each sample's segments were taken and kept in the furnace and the temperature of the furnace is set to the desired level and the power is turned ON. After the temperature of the furnace reaches the desired level, the samples are heated for an hour. After the heating is done, the samples are cooled at the normal cooling rate of the furnace. The samples after annealing at different temperatures are studied by XRD and Raman to see the crystallization of silicon. Tables 1, 2 & 3 below shows the deposition parameters of the samples.

Table 1 shows the deposition parameters for a-Si/Al/Sapphire.

Target Material	Crucible Used	Pressure inside Evaporator (torr)	Current (mA)	Voltage (KeV)	Rate of Deposition (A^0/Sec)	Thickness (nm)	Time (mins)
Al	Intermetallic	1.4×10^{-6}	52	7.17	0.22 - 0.64	100	50
Si	Molybdenum	1.8×10^{-6}	76	7.74	1.0 – 2.7	400	45

Table 2 shows the deposition parameters for a-Si/Ag/Sapphire.

Target Material	Crucible Used	Pressure inside Evaporator (torr)	Current (mA)	Voltage (KeV)	Rate of Deposition (A^0/Sec)	Thickness (nm)	Time (mins)
Ag	Molybdenum	3.2×10^{-6}	18	7.51	2.22 - 2.71	100	06
Si	Molybdenum	1.8×10^{-6}	76	7.74	1.0 – 2.7	400	45

Table 3 shows the deposition parameters for 250nm a-Si/Ag/Sapphire.

Target Material	Crucible Used	Pressure inside Evaporator (torr)	Current (mA)	Voltage (KeV)	Rate of Deposition (A^0/Sec)	Thickness (nm)	Time (mins)
Ag	Molybdenum	2.1 $\times 10^{-6}$	16	7.76	2.22 - 2.80	100	05
Si	Molybdenum	2.4 $\times 10^{-6}$	76	7.61	1.0 – 2.7	250	30

5.2 Results and Discussions

X-Ray Diffraction:

The X-Ray diffraction is used to study the crystallization of the silicon. The results obtained from XRD are discussed below. Let us first discuss about the XRD plot of the a-Si/Al/Sapphire which is not annealed. The Fig 5.4 shows us two high peaks. These peaks are due to presence of Al_2O_3. Al_2O_3 is substrate. So, the peaks which we see are substrate peaks. We are more interested at the peaks of crystalline silicon. The standards followed by XRD say that the silicon peaks appears at around 28 degrees. So, we will not discuss about the other peaks present in the XRD plots and mainly concentrate on the plots with 2 theta angle at the range of 21-30 degrees.

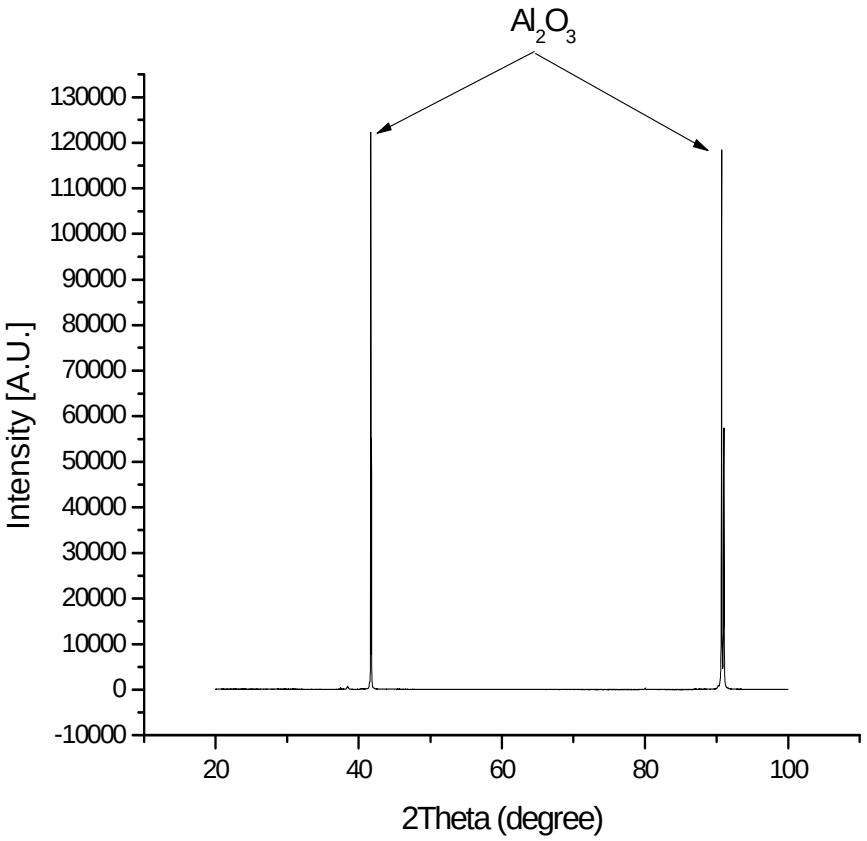

Figure 5.4 X-Ray diffraction plot of Un-annealed a-Si/Al/Sapphire sample.

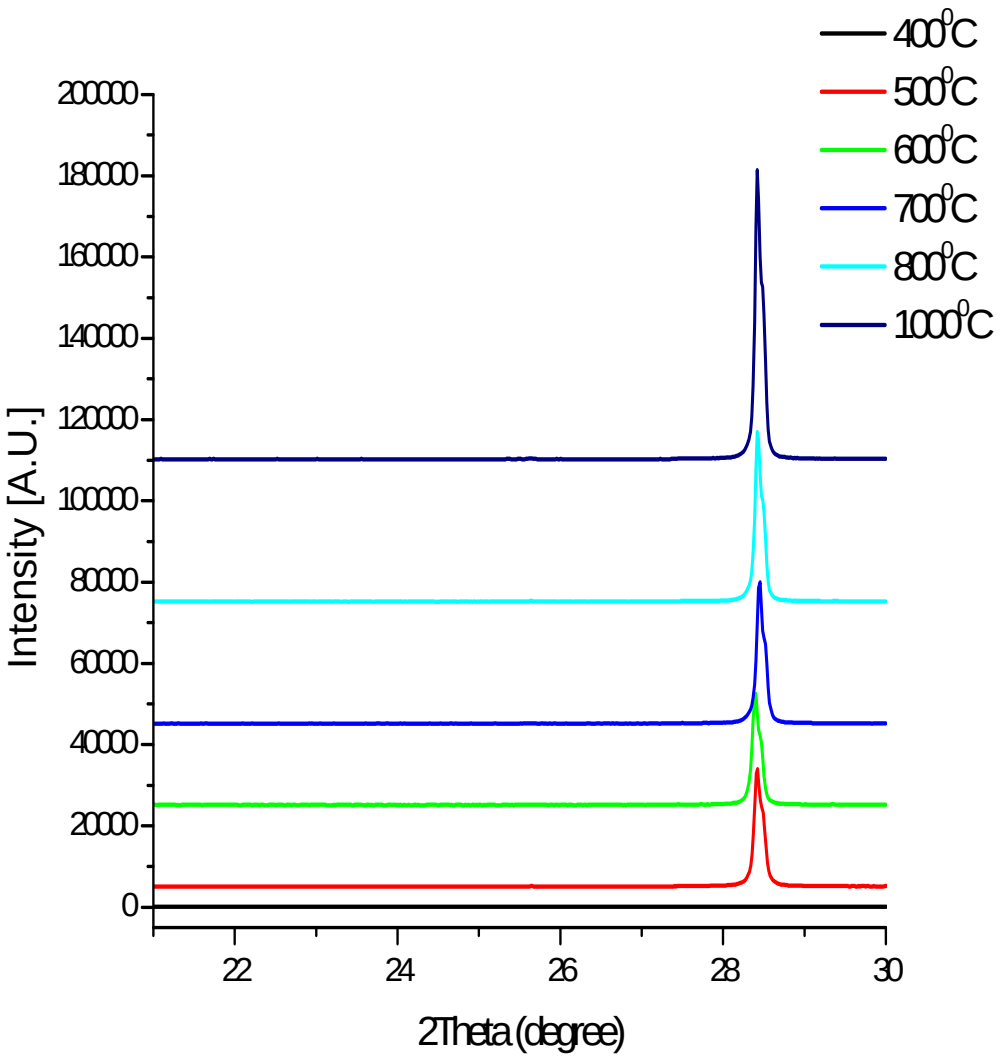

Figure 5.5 XRD plots of a-Si/Al/Sapphire sample annealed at different temperatures.

Figure 5.5 shows the XRD plots of a-Si/Al/Sapphire sample at different temperatures. We can see from the graphs that at high temperature annealed samples show the high peaks when compared with the lower temperature annealed samples. As we can see from the Fig 5.5, the peak of silicon was not seen at 400^0C. The crystalline silicon peak

appears at 500^0C. This implies that the crystallization was started at around 500^0C or may be less.

Fig 5.6 shows the XRD plots for a-Si/Ag/Sapphire sample annealed at different temperatures. Due to different metal used in this sample when compared with previous sample, the crystallization temperature for silicon is different. In Fig 5.6, the peak resembling silicon only started at 600^0C . At 600^0C we see a small peak which resembles silicon peak. So the crystallization of silicon with silver as metal used has a crystallization temperature at 600^0C . This when compared to Al proves that Al has less crystallization temperature(less than 500^0C).

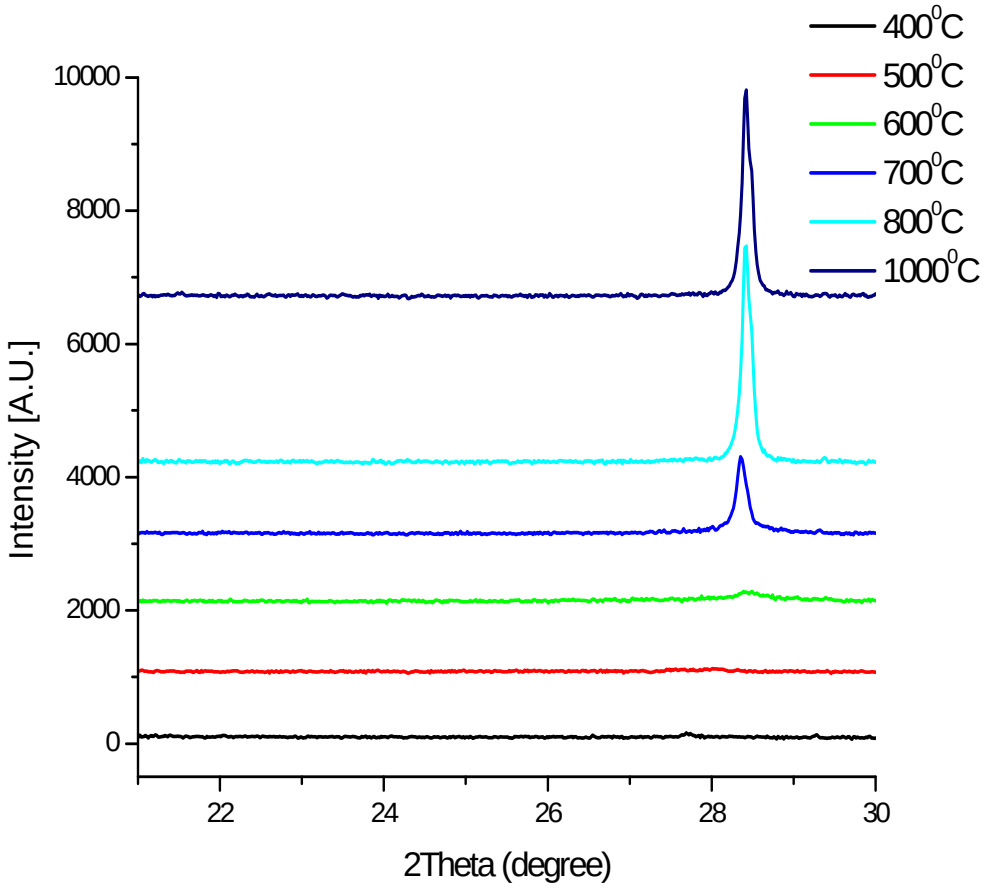

Figure 5.6 XRD plots of a-Si/Ag/Sapphire sample annealed at different temperatures.

Fig. 5.7 shows the XRD results of 250nm a-Si/Ag/Sapphire sample annealed at different temperatures. We can see from the figure that crystallization started at 500^0C which is less when compared with a-Si/Ag/Sapphire. The graphs at high temperatures show almost the same peaks; this is because almost all the silicon present on the sample is crystallized. There is not much difference in the peaks of higher temperature annealed samples.

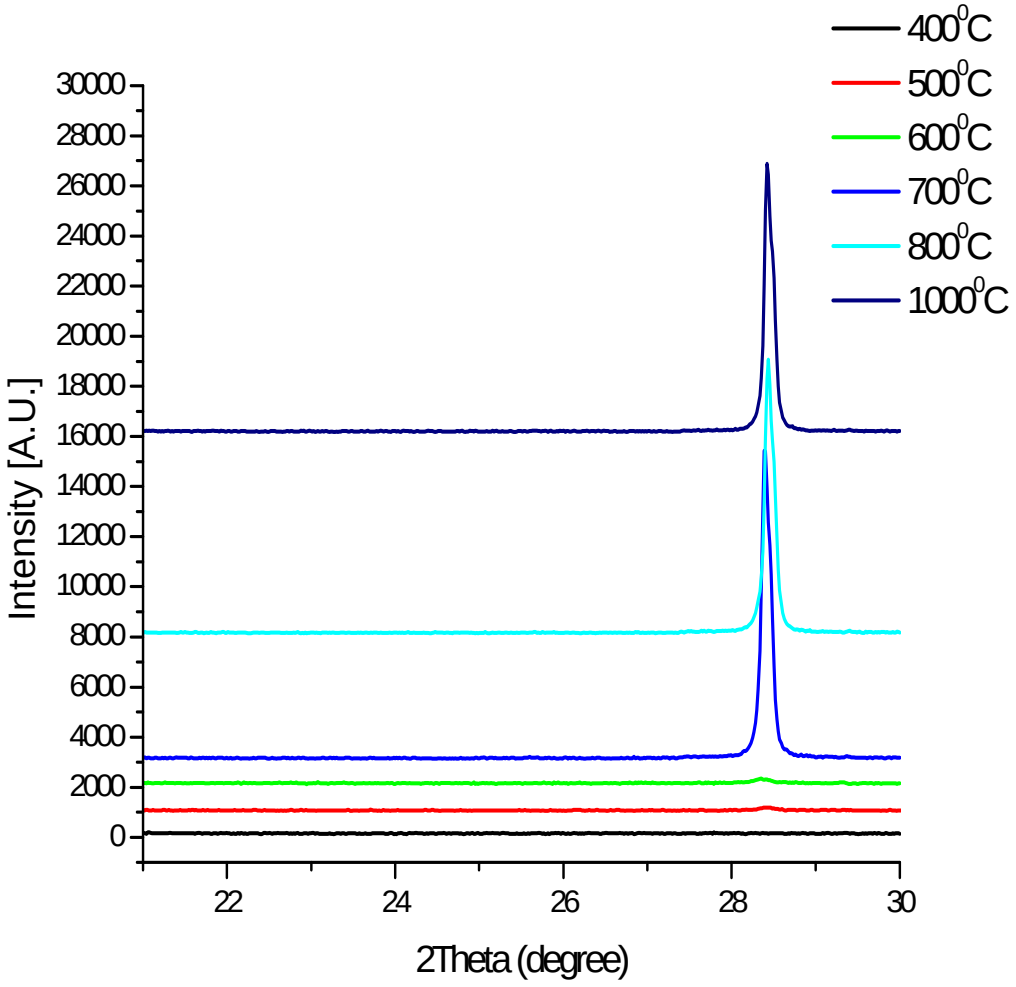

Figure 5.7 XRD plots of 250nm a-Si/Ag/Sapphire sample annealed at different temperatures.

Raman:

The samples were also studied in Raman spectrometer. The results from both methods were almost agreed with each other. The Fig 5.8 shows us the Raman shift for the a-Si/Al/Sapphire sample at different temperatures. As the temperatures were increased the sharp peak for the silicon was increased. At low temperatures we cannot see any peaks that mean that there was no crystallized silicon present. We can see from Fig 5.8, the peak for silicon started at 500^0C . So the crystallization of the a-Si/Al/Sapphire started at 500^0C .

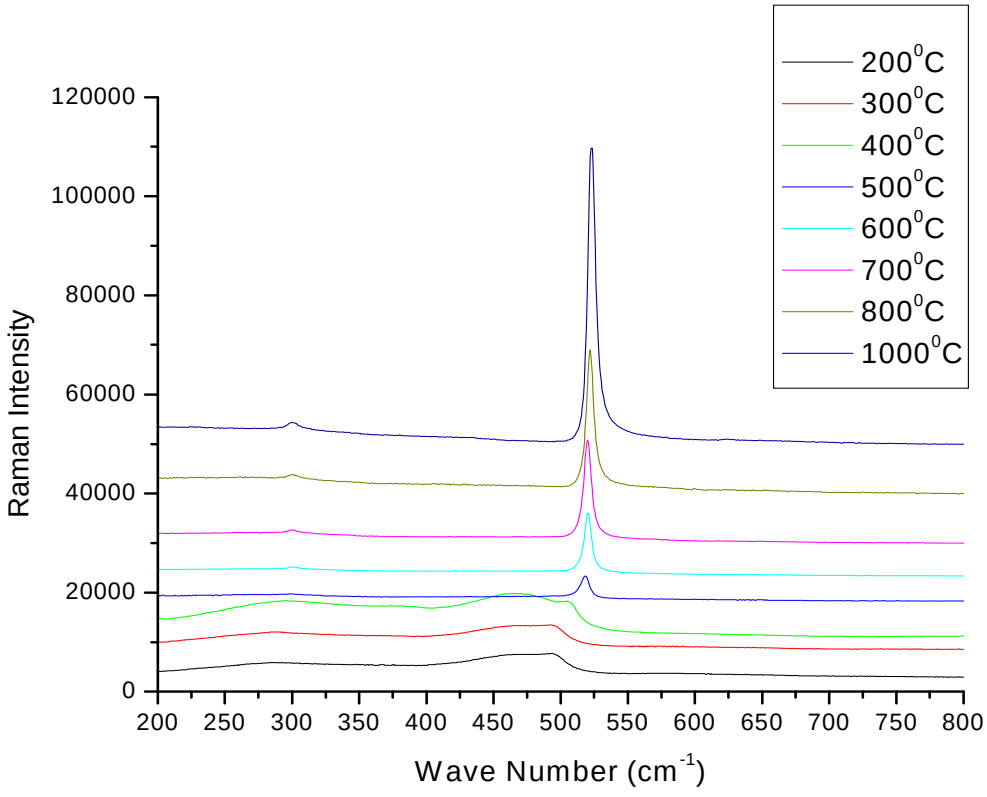

Figure 5.8 Raman plots for a-Si/Al/Sapphire sample annealed at different temperatures.

In Fig 5.9 we can see for a-Si/Ag/Sapphire sample the crystallization started at 600^0C. As the temperature increases the peak in the graph also increased. This shows that the more and more of silicon is being crystallized.

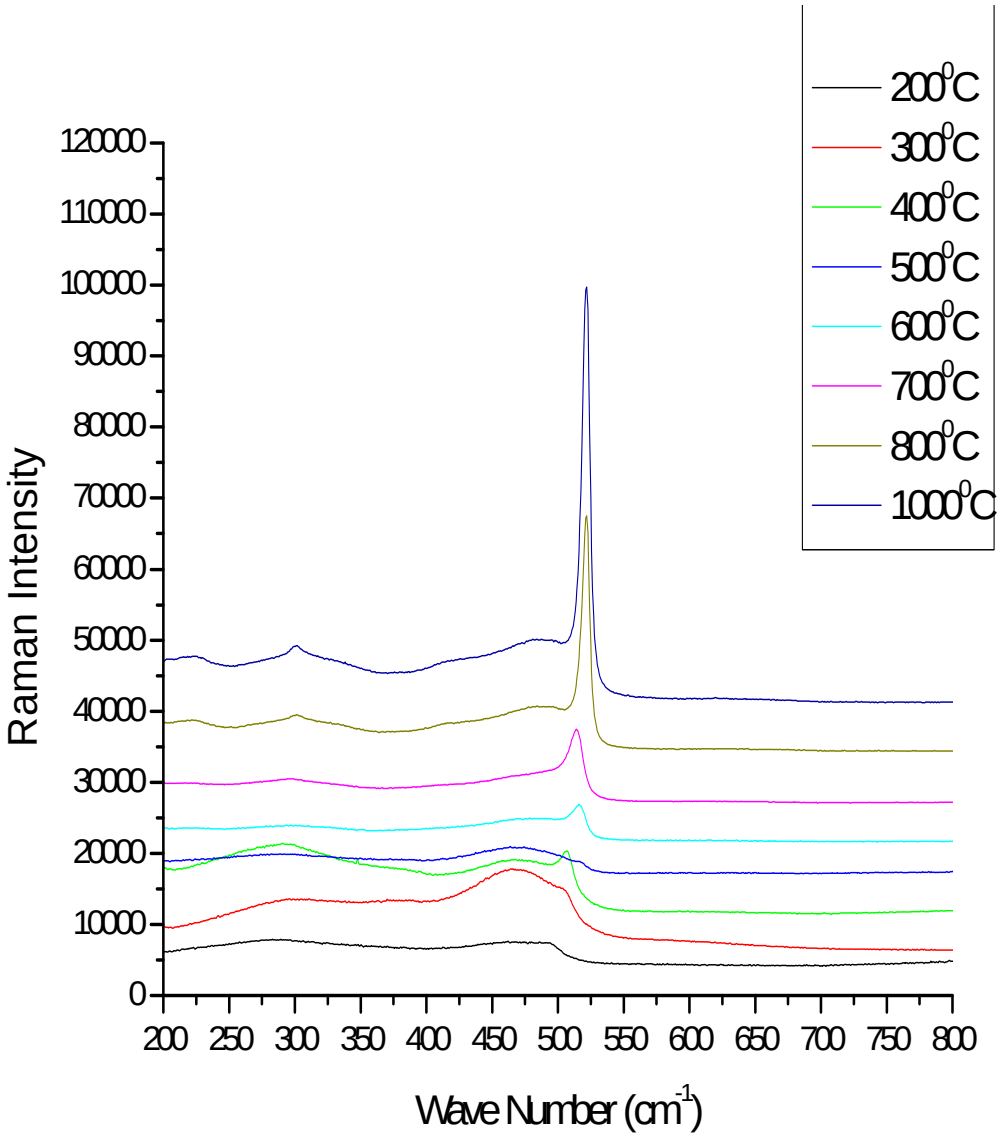

Figure 5.9 Raman plots for a-Si/Ag/Sapphire sample annealed at different temperatures.

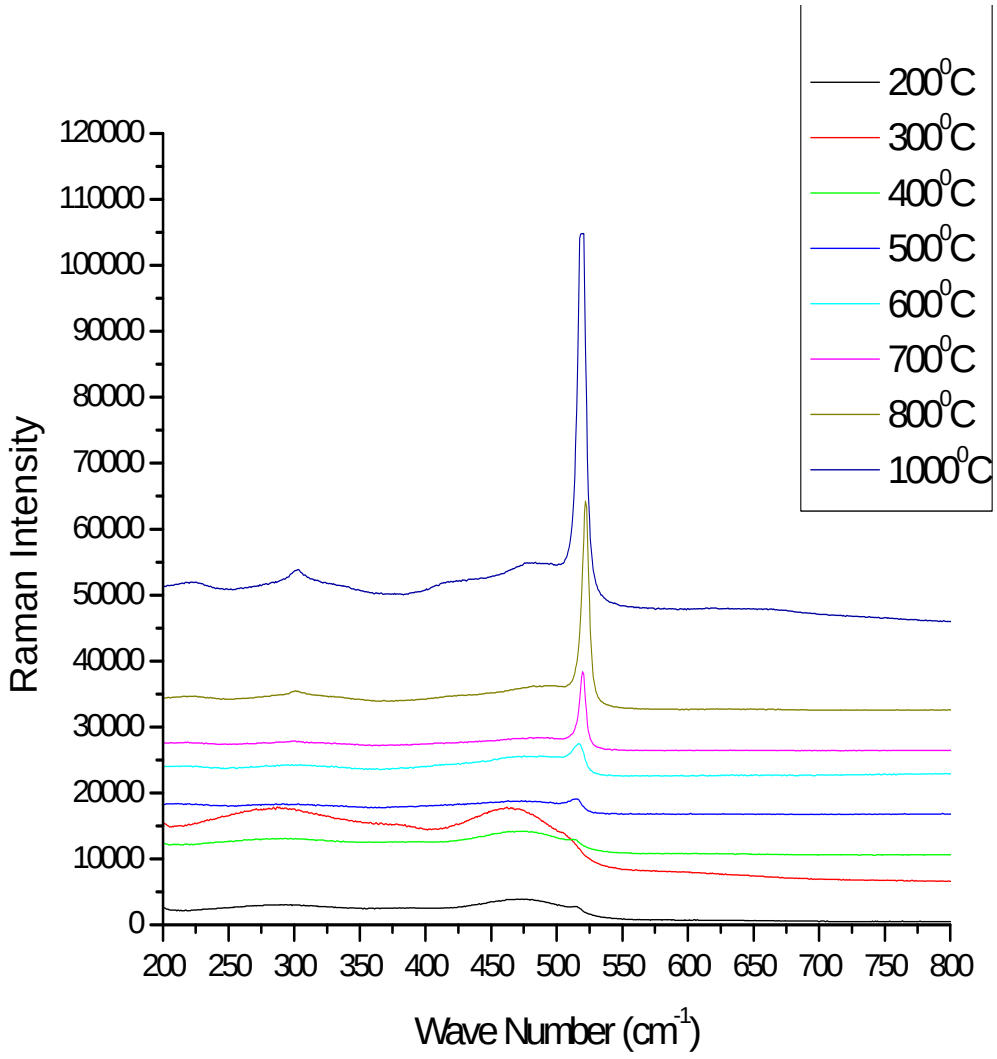

Figure 5.10 Raman plots for 250nm a-Si/Ag/Sapphire sample annealed at different temperatures.

Fig 5.10 shows the graph from Raman spectroscopy for 250nm a-Si/Ag/Sapphire sample. These results are different from the previous sample a-Si/Ag/Sapphire. The thicknesses of silicon, deposited on these samples are different. For a-Si/Ag/Sapphire sample, thickness of deposited silicon is 400nm. The 250nm a-Si/Ag/Sapphire sample has silicon thickness of 250nm. Due to this variation of thickness we can find difference in crystallization temperature. Due to less thickness in 250nm a-Si/Ag/Sapphire sample, the crystallization started little sooner than for a-Si/Ag/Sapphire sample. It just started to crystallize at 500^0C whereas 250nm a-Si/Ag/Sapphire sample started to crystallize at 600^0C. When comparing the Fig 5.8 and 5.10, both the samples started to crystallize at same temperature but the peak for a-Si/Al/Sapphire sample is higher than 250nm a-Si/Ag/Sapphire sample. So this proves that the Al is better when compared with Ag to reduce the crystallization temperature of silicon thin films.

CHAPTER 6

CONCLUSION AND RECOMMENDATION

6.1 Conclusion

High purity samples were obtained from the E-beam deposition system in Nevada Nanotechnology lab and these samples were annealed at different temperatures. The annealed samples were then studied with two methods, X-ray diffraction and Raman spectroscopy. The results show that at low temperatures the silicon is crystallized. We studied the crystallization of silicon with two different metals Al, and Ag. They both showed different crystallization temperatures. Al is better when compared with Ag for crystallization. Aluminum induced crystallization showed low temperature crystallization at around 500^0C. But for silver induced crystallization, the silicon started to crystallize at 600^0C. Due to low temperature crystallization of thin film silicon is important for many industrial applications such as flat panel displays and silicon solar cells. Metal induced crystallization of a-Si leads to the formation of continuous poly-Si films with good crystallinity according to the XRD and Raman experiments. Due to low process temperature and short crystallization time, low-cost substrates can be used for solar cells. This reduces the overall cost of the solar cells. High purity crystalline silicon thing films were obtained.

6.2 Recommendations

This process and study can be done with different metals like Tin and Lead, to see, whether crystallization temperature is lowered than the aluminum induced crystallization. Instead of metal layer, the nanoparticle deposition of metals can also be done and after annealing, the crystallization temperature of silicon can be studied.

REFERENCES

[1] Sposili, R. S. and Im, J. S. "Sequential Lateral Solidification of Thin Silicon on SiO2." *Appl. Phys. Lett*., 69 (1996), 2864-2868.

[2] Spinella, C., Lombardo S., and Priolo F. "Crystal Grain Nucleation in Amorphous Silicon." *J. Appl. Phys*., 84 (1998), 5383-5414.

[3] R.B. Bergmann, G. Oswald, M. Albrecht, V. Gross, Solar Energy Mater. Solar Cells 46 (1997) 147.

[4] K. Ishikawa, M. Ozawa, C.-H. Oh, M. Matsumura, Jpn. J. Appl. Phys. 37 (1998)731.

[5] Hultman, L., Robertsson, A., Hentzell, H., Engstrom, J. and Psaras, P. "Crystallization of Amorphous Silicon During Thin Film Gold Reaction." *J. Appl. Phys*., 62 (1987), 3647-3655.

[6] http://www.icmm.csic.es/fis/english/evaporacion_electrones.html

[7] Liu G, Fonasho SJ. Appl Phys Lett 1989;55:660.

[8] Nemanichi RJ, Fulks RT, Stafoord BL, Vanderplas HA. J Vac Sci Technol A 1985;3:938.

[9] Kawazu Y, Kudo H, Onari S, Arai T. Jpn J. Appl Phys 1990;29:2698.

[10] Hayzelden C, Bastone JL. J Appl Phys 1993;73(12):8279.

[11] Hempel T, Schoenfeld O. Solid State Communication 1993;85(1):921.

[12] Russell SW, Li J, Mayer JW. J Appl Phys 1991;70(9):5153.

[13] Nast O, Wenham SR. J Appl Phys 2000;88(1):124.

[14] Haque MS, Naseem HA, Brown WD. J Appl Phys 1994;75:3928.

[15] C. Detavernier, C. Lavoie, F. d'Heurle, H. Bender, R. Van Meirhaeghe, J. Appl. Phys. 95 (2004) 5340.

[16] Z. Jin, G. Bhat, M. Yeung, H. Kwok, M. Wong, J. Appl. Phys. 84 (1998)194.

[17] http://serc.carleton.edu/research_education/geochemsheets/techniques/XRD.html

[18] http://www.physics.pdx.edu

[19] http://www.panalytical.com

[20] http://www.horiba.com/scientific/products/raman-spectroscopy/raman resource/raman-tutorial/

[21] http://en.wikipedia.org/wiki/Raman_spectroscopy

[22] C. Hayzelden, J. Batstone, J. Appl. Phys. 73 (1993) 8279.

[23] K. Kim, S. Park, S. Kim, J. Jang, J. Non-Cryst. Solids 352 (2006) 976.

[24] J. Jang, J. Oh, S. Kim, Y. Choi, S. Yoon, C. Kim, Nature 395 (1998) 481.

[25] J. McCaldin, H. Sankur, Appl. Phys. Lett 20 (1972) 171.

[26] S. Yoon, S. Park, K. Kim, J. Jang, Thin Solid Films 383 (2001) 34.

[27] S-W. Lee, Y-C. Jeon, S-K. Joo, Appl. Phys. Lett. 66 (1995) 1671.

[28] O. Nast, S. Brehme, S. Pritchard, A.G. Aberle, S.R. Wenham, Sol. Energy Mater.Sol. Cells 65 (2001) 385.

[29] C.H. Yu, P.H. Yeh, L.J. Chen, Nucl. Instr. Meth. Phys. Rev. B 237(2005) 167.

[30] T. Sameshima, K. Ozaki, N. Andoh, Appl. Phys. A 71 (2000)1.

[31] D.-K. Choi, H.-C. Kim, Y.-B. Kim, Appl. Phys. Lett. 87 (2005) 063108.

[32] I.-H. Hong et al., Nucl. Instr. Meth. Phys. Res. A 467/468 (2001) 905.

VITA

Graduate College
University of Nevada, Las Vegas

Sandeep Kumar Raju Sangaraju

Degrees:

Bachelor of Technology, Electronics and Communication Engineering, 2007
J.N.T University, Hyderabad, India

Thesis Title: Metal Induced Crystallization of Silicon Thin Films

Thesis Examination Committee:

Chairperson, Dr. Biswajit Das, Ph.D, P.E.
Committee Member, Dr. Yingtao Jiang, Ph.D
Committee Member, Dr. Mei Yang, Ph.D
Graduate Faculty Representative, Dr. Frank van Breukelen, Ph.D